CrossMark

Comparison of chemical and physical reduction methods to prepare layered graphene by graphene oxide: optimization of the structural properties and tuning of energy band gap

M.-S. Poorali[1] · M.-M. Bagheri-Mohagheghi[1]

Abstract A systematic study to optimize the structural properties of graphene synthesized from modified graphene by both chemical and physical reduction methods were studied. In the chemical method, the two most common reducing agent hydrazine hydrate and sodium borohydride at different concentrations were used. In the physical method, two different samples were produced using a heat treatment at 200 °C in the presence of argon gas. Structural properties, morphology and functional groups of samples by SEM, TEM, XRD, FTIR, UV–Vis, PL and TGA were analyzed. The results show that graphene sheets have been produced in all methods. This study showed that modified graphene with hydrazine hydrate (3 ml per 100 mg of GO) has the best structural properties. The result of physical reduction method by heat treatment in argon gas showed the lowest energy gap among other samples. The PL emission spectroscopy showed the strong intensities at 500 and 600 nm due to the overlap of the second order emissions in the electron–hole recombination processes as results from different types of electronically excited states and physical reduction had minimum of intensity. The obtained graphene nano-sheets showed an energy band gap from 1.37 to 2.70 eV that is suggested as an application method in opening of the energy band gap. However, synthesized graphene by the chemical reduction method by hydrazine hydrate treatment has the better structure, but the physical reduction method is rapid and equally appropriate.

✉ M.-M. Bagheri-Mohagheghi
bmohagheghi@du.ac.ir

[1] School of Physics, Damghan University, Damghan, Iran

1 Introduction

Graphene, an exciting material [1] that is a single layer of carbon atoms bonded together in a hexagonal lattice, has emerged in recent years as a novel and important class of materials on its own merit. This is due not only to the plethora of new fundamental science that it has displayed [1] but also to the prospect of a variety of applications that span graphene-based nanoelectronic devices [2], composite materials [3], and gas sensors [4] as well as energy-storage materials [5], and "paper-like" materials [6]. The remarkable properties of graphene reported so far include high values of its Young's modulus (~ 1100 GPa) [7], thermal conductivity (~ 5000 W m^{-1} K^{-1}) [8], mobility of charge carriers (200,000 cm^2 V^{-1} s^{-1}) [9] and specific surface area (calculated value, 2630 m^2 g^{-1}) [5].

As with any new material that is intended for large-scale applications, the development of methods that allow the mass production and processing of graphene sheets has become a top priority. The development of various methods for producing graphene has stimulated a vast amount of research in recent years [1]. Graphene has been made by four different methods. The first method is chemical vapor deposition (CVD) [10]. The second one is the micromechanical exfoliation of graphite [11]. The third one is epitaxial growth on SiC [12] and the fourth one is the creation of colloidal suspensions. In this regard, although the originally reported approach to the preparation of graphene (i.e., micromechanical cleavage of bulk graphite) leads to small samples and high-quality 2D crystals and is suitable for fundamental studies, it suffers from extremely low productivity and is therefore inadequate for large-scale use [1].

At present, the only route that affords graphene-based sheets in considerable quantities relies on the chemical

conversion of graphite to graphite oxide (GO) [3]. GO offers potential for the production of chemically modified graphene on the large-scale [13]. GO has emerged as a precursor offering the potential of cost effective production of graphene-based materials. GO has been mainly produced by the Brodie [14], Staudenmaier [15] and Hummers [16, 17] methods. All three methods involve oxidation of graphite in the presence of strong acids and oxidants. The level of the oxidation can be varied on the basis of the method, the reaction conditions and the precursor graphite used.

GO consists of a layered structure of 'graphene oxide' sheets that are strongly hydrophilic such that intercalation of water molecules between the layers readily occurs [18]. Notably, graphite oxide can be completely exfoliated to produce aqueous colloidal suspensions of graphene oxide sheets by simple sonication for a long enough time [19]. This provides a very convenient setting for the implementation of solution-phase techniques toward the conversion of graphene oxide back to graphene by way of chemical reduction or the processing of the graphene oxide sheets into films and paper like materials [20]. The reduction of the graphene oxide by chemical methods using reductants such as hydrazine hydrate [21], sodium borohydride [22] and thermal methods [23] produce electrically conducting modified graphene.

In the present work, structural comparison of graphene sheets obtained by the two different methods for the reduction of graphene oxide has been investigated, chemical reduction process and physical regeneration through heat treatment. Reduction of graphene oxide by hydrazine hydrate and sodium borohydride is the most common and one of the strongest reductions with three different molar concentrations was performed, and the physical reduction of graphene oxide by heating in argon atmosphere to obtain graphene powder was performed. Their morphology and microstructural characteristics were studied in detail.

2 Experimental procedures

In the present work, eight samples of graphene were prepared with reduce method. The three samples HMG1, HMG2 and HMG3 were prepared by chemical reduction method using "hydrazine hydrate". To prepare the three samples BMG1, BMG2 and BMG3, chemical reduction method using "sodium borohydride" were used, and two next samples AMG and ACMG were prepared by physical reduction method by heat treatment in the presence of "argon gas".

2.1 Synthesis of graphene oxide

Hummers method [17] was used for the synthesis of GO. The amount of 96 ml of concentrated sulfuric acid to a mixture of 3 g of graphite powder with 1.5 g of $NaNO_3$ was added, and the mixture using an ice bath was cooled to 0 °C. $KMnO_4$ (9 g) was added slowly to the mixture so that the temperature remains below 20 °C. The reaction was heated to 35 °C, and was stirred at the same temperature for 7 h. To increase the oxidation of graphite, the amount of additional 9 g $KMnO_4$ was added to the mixture in one portion, and the reaction was stirred at the same temperature for 12 h. The reaction mixture was cooled to room temperature and poured onto ice (400 ml) with 30 % H_2O_2 (3 ml). Mixture with multiple filtering, centrifuging, decanting and washing was purified according to the following steps. The mixture was centrifuged (4000 rpm for 4 h), and the supernatant was decanted away. The remaining solid material was then washed in succession with 200 ml of deionized water, 200 ml 30 % HCl and twice with 200 ml of ethanol.

2.2 Chemical reduction with hydrazine hydrate

The chemical reduction of graphene oxide with hydrazine hydrate [17, 24] was performed to produce three different samples according to the following steps. 100 mg of graphite oxide in 100 ml of deionized water for 1 h was dispersing. Then, in the sample HMG1, 1 ml of hydrazine hydrate was added to the mixture. Mixture in an oil bath at 95 °C for 60 min in the presence of argon gas was reflux. After, the mixture was left black. The mixture was left overnight. Then the mixture was filtered and washed three times with deionized water and three times with ethanol, and the remaining precipitate was dried under vacuum and at room temperature for 2 h. To prepare samples HMG2 and HMG3 respectively amount of 3 and 6 ml of hydrazine hydrate was added to the mixture, and the process was repeated as in the first sample.

2.3 Chemical reduction with sodium borohydride

The other three samples were produced using chemical reduction of graphene oxide by sodium borohydride [25]. BMG1 was prepared according to the following steps. 150 mg of GO in 150 ml of deionized water for 1 h were dispersing. Then 800 mg sodium was dissolved in 30 ml deionized water was added to the mixture. Finally, the prepared mixture for 60 min at T = 90 °C in oil bath under argon was reflux. After, the mixture was left black. The mixture was left overnight. As the first sample, the mixture was filtered and washed three times with deionized water

and three times with ethanol, and the remaining precipitate was dried under vacuum and at room temperature for 2 h. In two other samples BMG2 and BMG3 respectively, amount of 1.2 and 1.6 g of sodium borohydride was dissolved in 30 ml water, and then it was added to the mixture, and the process was repeated as in the first sample.

2.4 Physical reduction by heat treatment under argon gas flow

AMG and ACMG samples were prepared by reduction by heat treatment [17, 26] according to the following steps. For this purpose, in AMG 100 mg of graphite oxide was placed in the medium part of a quartz reactor under argon gas flow at a rate of 20 ml min^{-1} for 30 min at 200 °C. This was associated with CO, CO_2 and H_2O gas sublimation. In this way, GO lost 90 % of its weight. For ACMG preparation, 0.2 g of the HMG3 in the presence of argon gas for 30 min at 200 °C was placed.

3 Characterization

X-ray diffraction system (BRUKER, D8 Advance, Germany) was used for the X-ray analysis with Cu-Kα radiation ($\lambda = 1.540$ Å). Step scanning was done with 2θ intervals from 4° to 60°. UV–Vis spectroscopy was used for the measurement of absorbance to find the electronic structure of the samples in the wavelength range of 200–1100 nm. Fourier transform infrared spectra were recorded using spectrum one: FTIR-spectrometer in the range 500–4000 cm^{-1} to characterize the functional groups. The morphology of the materials was investigated. To further know its morphology at a higher magnification, field emission scanning electron microscope (FE-SEM) analysis was carried out for all samples. Transmission electron microscopy (TEM) images were recorded. For TEM analysis, samples were suspended in water via ultrasonication for 2 h and then the unstable dispersion was dropped on a fresh lacey carbon TEM grid. Thermal stability of the sample was studied by thermo gravimetric analysis (TGA) up to 600 °C with a heating rate of 10 °C min^{-1} under argon atmosphere. Photoluminescence (PL) measurement was performed at room temperature.

4 Results and discussion

4.1 Graphene oxide and graphene dispersions

The reduction of GO can be deduced from the color change of the GO dispersion before and after reaction. Figure 1 shows the color of GO and some modified samples changes from yellow brown to black when it was stirred in distilled water 30 min. This shows that the used methods were effective in the reduction of graphene oxide. The hydrazine hydrate was more effective in the reduction of graphene oxide. In other samples, part of the graphene oxide without reduction remains.

4.2 Structural analysis by XRD

XRD was used to the structural characterization of the few-layered graphene nano-sheets. We compared the structural properties of the graphene nano-sheets synthesized with different methods, in accordance with the above description, and GO obtained by Hummers method by studying the powder X-ray diffraction patterns. In Fig. 2, the characteristic reflection (002) of all the samples can be compared in order to understand the influence of various syntheses in structure. The sharp peak at 2θ = 26.7° indicates a highly organized crystal structure with an d-space = 0.34 nm, which is consistent with the layer spacing of normal graphite [27]. This occurs because the interlayer spacing inside the few-layered graphene nano-sheet has a structure similar to that of normal graphite.

As the patterns show, the XRD pattern of the graphene sheets obtained with hydrazine hydrate (HMG1-2–3), and AMG have more sharp peak than the others at 2θ = 26.7°, which imply better crystallinity. Compared with pristine graphite (not shown), it can be clearly observed that the diffraction (001) peak of GO appear at 2θ = 9.84°. Using the Bragg equation, the distance between the plates is obtained 0.89 nm. This value is larger than the distance between graphite plates. This is due to a result of intercalation of water molecules and the formation of functional groups containing oxygen during oxidation of the graphite layers [17].

There are rather weak peaks at about 2θ = 9° in the rest sample. This peak is similar to the typical (001) diffraction peak of graphene oxide (GO) [17]. In the samples synthesized with hydrazine hydrate (HMG1-2–3) and ACMG, this peak is relatively weak but in the samples synthesized with sodium borohydride (BMG1-2–3), and AMG is relatively larger than the others. This indicates that modified graphene sheets in (HMG1-2–3), and ACMG samples are of higher purity than (BMG1-2–3) and AMG due to elimination of oxygen-containing functional groups. Based on experimental and simulated results [28, 29], the broad peak at 2θ = 24.7° can be ascribed to their few-layer nanostructures and could also be due to the complicated nature of the size, curvature, sheet rotation, and atom positioning in the graphene sheets.

The broad peak at 2θ = 20.1°, suggests the existence of regions of expanded stacking of more corrugated or disordered graphene sheets, probably existing at the edge

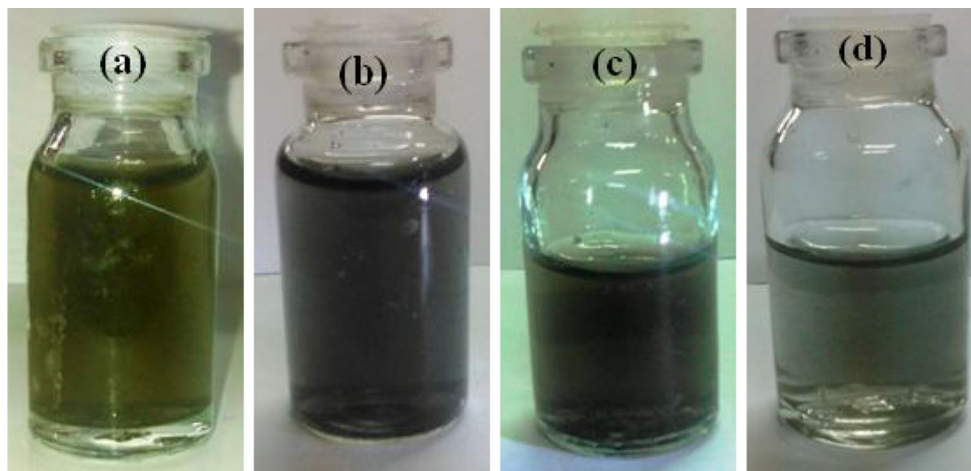**Fig. 1** Digital photographs of aqueous dispersions of **a** GO, **b** HMG3, **c** BMG2, **d** AMG
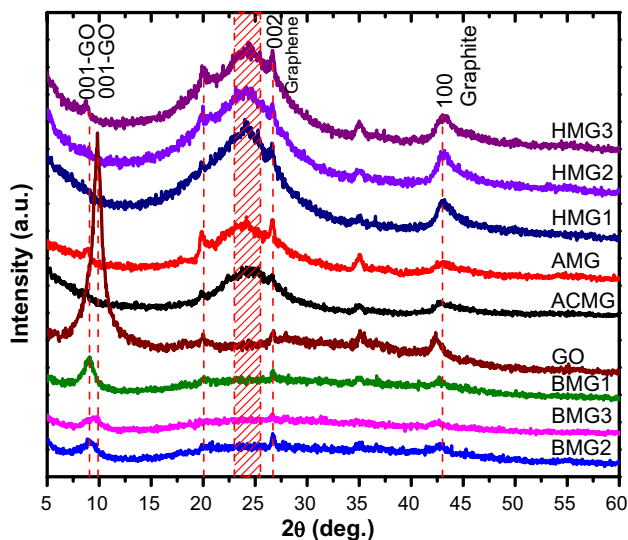

Fig. 2 XRD spectra of samples (1.54 Å Cu Kα1 as wavelength)

areas [27]. Generally, crystal lattice is formed better, and oxygen-containing functional groups are removed better in HMG1-2–3 samples. In other words, the chemical reduction by hydrazine hydrate treatment is better to remove oxygenated groups. The heat treatment effectively eliminated the oxygen-containing groups, but quality of crystal structure declined slightly in ACMG sample. In contrast, sodium borohydride to remove oxygen groups than others did not perform well as well as the quality of the resulting crystal structure is not good. In Table 1, the intensity and location of the peaks of different samples were compared with each other.

4.3 SEM analysis

Figure 3 show the scanning electron microscopy (SEM) images of the some samples. SEM images of GO (Fig. 3a)

confirms the formation of layered graphene oxide structure that this sample used in the production of all other samples. Figure 3b–h shows the wrinkled structure of graphene layers. Almost similar morphology for samples generated by both physical and chemical reduction route can be seen.

4.4 TEM analysis

Graphene morphology for HMG1, AMG and BMG3 was characterized using TEM. The TEM images of these samples are shown in Fig. 4. A large sheet of graphene with several hundred nanometers dimensions found on the top of the grid, where it can be seen that there are wrinkled and transparent areas in the images. According to previous articles, wrinkled areas are part of the intrinsic nature of graphene, that becoming stable via bending [30]. It can be seen from TEM image shown in Fig. 4, that part of the graphene sheet shows relative flat morphology with low contrast, which is an indication of few-layer thickness. In all cases, the formation of graphene sheets can be seen.

4.5 FT-IR analysis

FT-IR spectroscopy was also given to study the functional groups on the surface of GO and graphene sheets obtained with different methods as shown in Fig. 5. The FT-IR spectra of the GO shows the absorption bands at 3420 (hydroxyl) and 1395 cm^{-1} (carboxyl), the C=O at 1730 cm^{-1}, C–O (carbonyl) at 1037 cm^{-1}, and absorption band at 1629 which can be assigned to the vibrations of the adsorbed water molecules and may also contain components from the skeletal vibrations of un-oxidized graphitic domains consistent with previous infrared spectra of GO [31–34]. This indicates that the oxygen functional groups were bonded to carbon molecules after oxidation. Thus,

Table 1 Comparison of the intensity peaks of the samples obtained from XRD pattern

2θ	Due to	GO	Chemical reduction						Physical reduction	
			HMG1	HMG2	HMG3	BMG1	BMG2	BMG3	AMG	ACMG
9.84°	Graphene oxide	o	n/o	n/o	d (8.75°)	d (9.75°)	d (8.98°)	d (9.05°)	d (8.82°)	n/o
20.1°	Defect the edge areas	o	o	i	i	n/o	o	o	i	o
24.7°	Complicated nature	n/o	o	o	o	n/o	n/o	n/o	o	o
26.7°	Similar to that of normal graphite (26.1)	o	i	i	i	o	i	i	i	o

The peak is observed [o], The peak is no observed [n/o]

The peak intensity is increased compared to the GO [i]

The peak intensity is decreased compared to the GO [d]

Numbers in parentheses show the peak displacement

similar to XRD, FTIR spectroscopy provided evidence of the presence of different types of oxygen functional groups on the graphene oxide.

It is clear from Fig. 5 that there are considerable changes in FT-IR spectra of GO after treatment with hydrazine hydrate and heat treatment. In these samples, after the chemical reduction of GO, the characteristic absorption bands of the oxygen-containing functional groups dramatically decrease, indicating that such GO has been reduced to graphene. According to Fig. 5 can be seen that the absorption bands at 1730 cm^{-1} (C=O) and at 1629 cm^{-1} (water molecules) in all three samples HMG1-2–3 have been removed. Furthermore, with increasing concentrations of hydrazine hydrate in HMG1-2–3 OH, epoxy and carbonyl groups are reduced. The samples synthesized with sodium borohydride minor changes have been made. In addition, it is observed that increasing the concentration of sodium borohydride in the samples BMG1-2-3, OH and carboxyl groups are decreased. This indicates that the oxygen-containing groups have not been omitted entirely. These results are in agreement with XRD results. Moreover, the peak at 1395 cm^{-1} shows that some of the carboxyl groups still exist after the reduction process except for AMG that is completely removed. These results suggest that treatment with hydrazine hydrate and heat treatment is a more effective method to remove oxygen-containing groups that commonly used. After reduction, the 1552 cm^{-1} peak has appeared in all samples, especially in the samples synthesized with hydrazine hydrate and heat treatment, which is related to the presence of C–C stretching in graphitic domains [35]. Changes in the FTIR spectrum are shown in Table 2.

According to the FTIR spectrum from graphene sample, the number of oxygen-containing groups remains on the surface of graphene. But due to the almost complete elimination GO peak in XRD pattern of graphene samples, the number of oxygen-containing groups on graphene samples is highly less than the number of oxygen-containing groups on the GO. Chemical or physical reduction reduces the oxygen-containing groups and thereby closing the gap, but they will not be completely eliminated and there is always unintended doping as reported in the other works [34–36]. Reduced GO always show p-type behavior at ambient conditions because of unintentional doping caused by residual species or oxygen molecules in environment [36].

4.6 TGA analysis

The TGA patterns of the samples are shown in Fig. 6 TGA curve of the AMG shows a negligible mass loss, which is only about 10 % of its total mass in the entire temperature range. AMG weight loss up to 300 °C is negligible and about 300–500 °C loses more weight. Synthesis of graphene sheets by the sodium borohydride treatment mass loss occurs in two stages, one in the temperature range of 0–300 °C appear, and the other is in the range of 300–500 °C, which is the thermal decomposition of labile functional groups containing oxygen and CO and CO_2 emissions is concerned [30].

Compared with BMG1–2, thermal stability of AMG, HMG1-2–3 are much higher, which indicates that the effective removal of oxygen-containing functional groups by treatment with hydrazine hydrate as the reducing agent. Also, In the ACMG, it can be seen that after annealing in the presence of argon gas is more thermally stable than BMG1-2. These results are consistent with XRD and FT-IR spectra. The TGA analysis showed high thermal stability for reduced sample with hydrazine hydrate at T = 500 °C.

4.7 UV–Vis analysis and calculation of optical band gap

Figure 7 shows UV–Vis spectra of the samples in the wavelength range 250–800 nm. The UV–Vis spectrum of

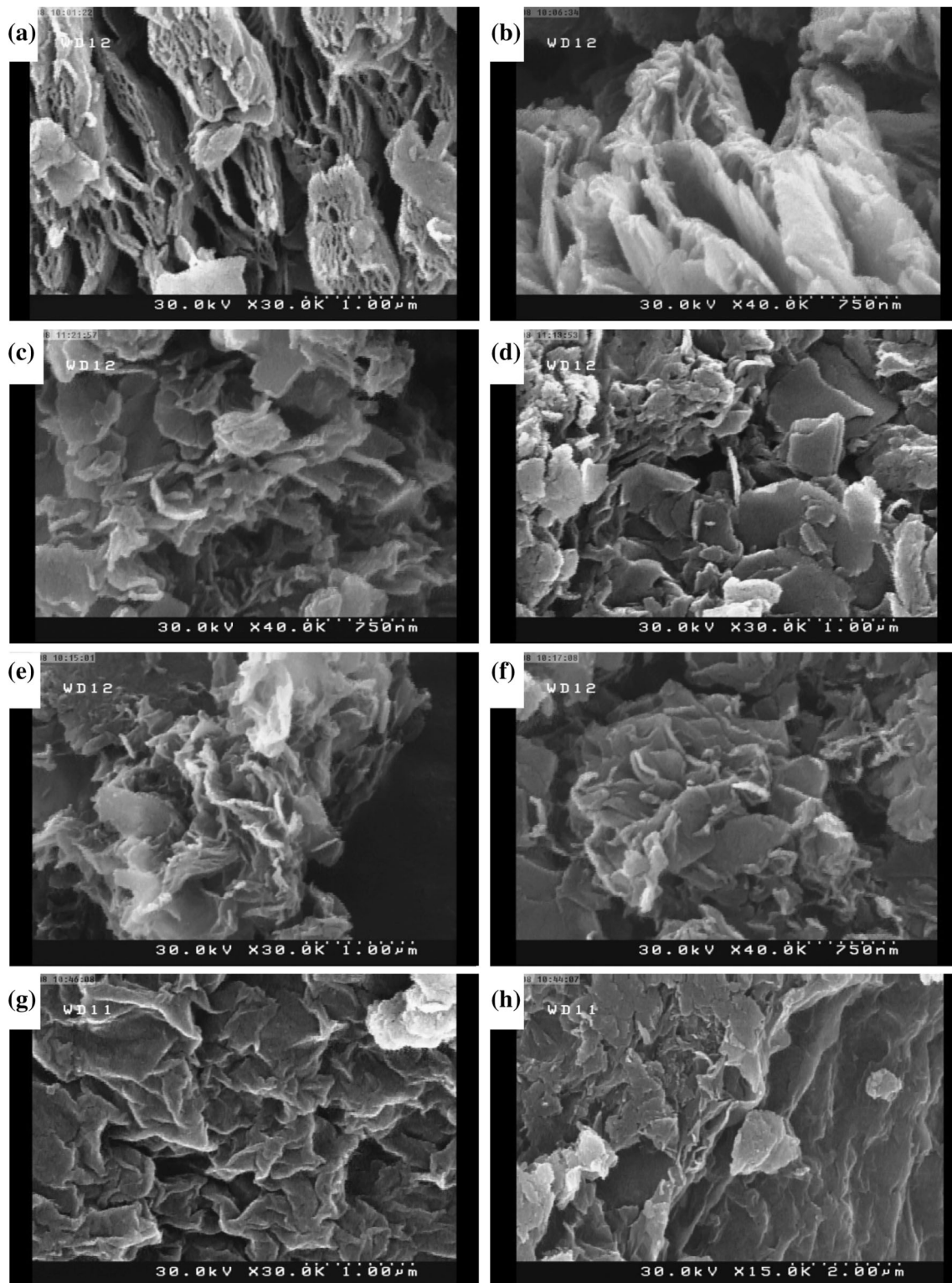Fig. 3 SEM image at different magnifications of the GO (**a**, **b**), ACMG (**c**, **d**), BMG2 (**e**, **f**), HMG3 (**g**, **h**)

graphene oxide exhibits one characteristic feature in this range that can be used as a means of identification. a maximum at ∼300 nm, which can be attributed to π–π

transitions of C=O bonds [17]. As shown in the UV–Vis spectrum, after the reduction of graphene oxide in all samples a weak peak of about 280 nm appears, that is
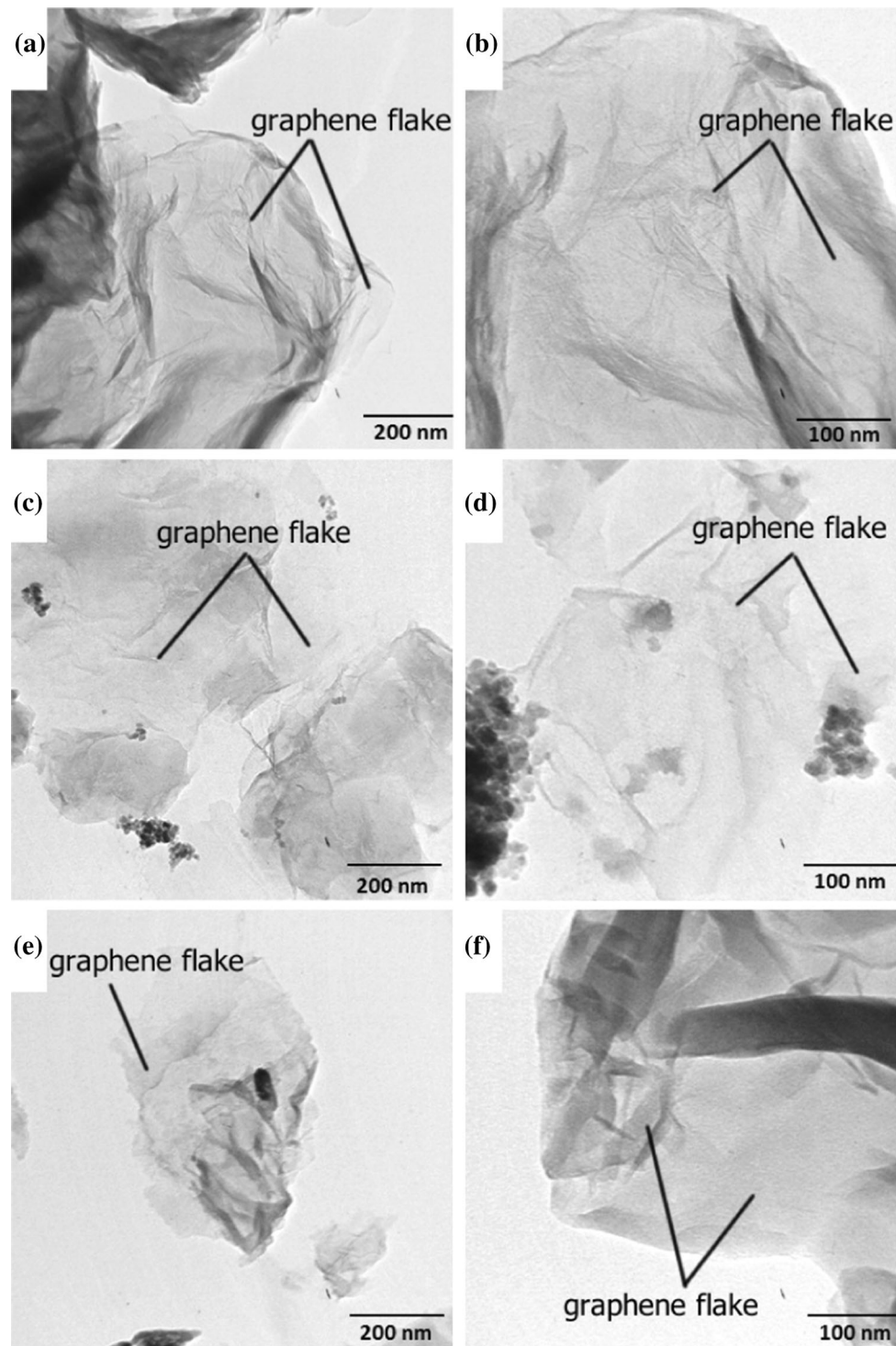
Fig. 4 TEM image at different magnifications of the AMG (**a**, **b**), BMG3 (**c**, **d**), HMG1 (**e**, **f**)

related to π–π^* transition of C–C bonds. It indicates that oxygen-containing groups on the GO surface are removed and the conjugated structure is restored.

Graphene has a zero energy gap; the energy gap in graphene opens by functional groups containing oxygen adsorption [36]. To calculate the energy gap of graphene
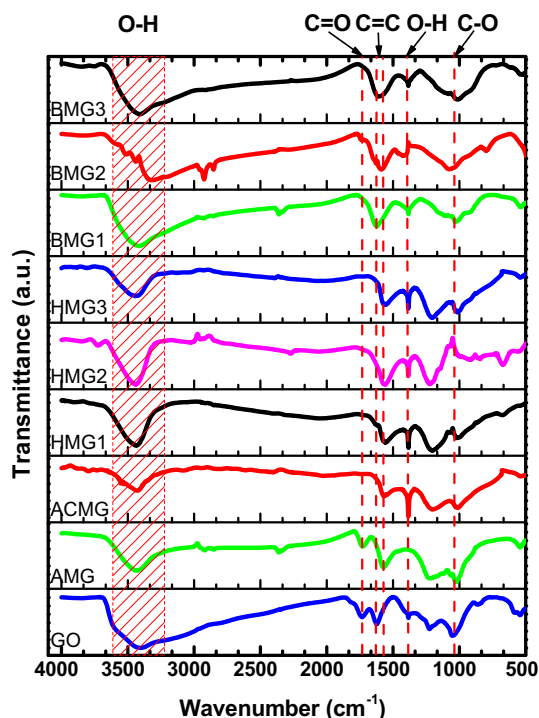
Fig. 5 FTIR spectrum of GO and modified graphene sheets

Fig. 6 TGA plot of GO and modified graphene sheets

sheets and therefore to compare the absorption of oxygen functional groups between samples, the UV–Vis spectroscopy was used. UV–Vis spectra of the samples was measured and used to calculate the direct band gap of graphene sheets, which is in agreement with previous papers [37]. The Tauc's equation [38, 39] was used to calculate the direct band gap of graphene sheets.

$$(\alpha h\nu)^2 \propto (h\nu - E_g) \quad (1)$$

where α is the absorption coefficient and it is calculated using UV–Vis spectra of the sample. Value of α is proportional to the absorbance of the sample. Also $h\nu$ is the photon energy and E_g is the band gap. For this purpose, the $(\alpha h\nu)^2$ curve was plotted on the $h\nu$ (Fig. 8) and by
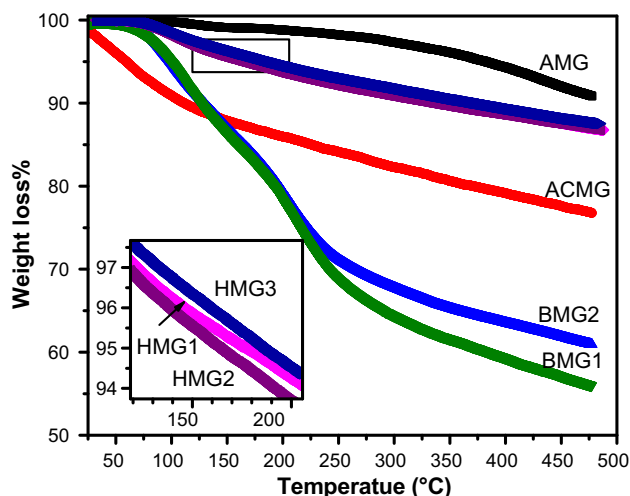
determining the intersection of the tangent line to the drastic change with the horizontal axis; the energy gap (E_g) of graphene sheets was obtained. Figure 9 shows the values of the energy band gap of graphene sheets, which is consistent with previous work [40]. These results indicate that functional groups containing oxygen adsorption open the band gap in graphene. GO has the highest oxygen functional groups, so its energy gap is the largest. By chemical reduction operations, functional groups on the graphene surface are removed, and the energy gap decreases. Figure 9 shows the samples prepared by hydrazine hydrate and heat treatment, have the best performance in the removal of the oxygen groups because of having the smallest gap. The samples were prepared by heat treatment on modified graphene sheets with hydrazine hydrate has the highest decrease in the band gap energy.

In Table 3 the results of analysis XRD, FTIR and calculate the band gap briefly presented. As it turns out the results are in good agreement with each other. According to Table 3, it follows that HMG2 had the best quality for

Table 2 The observed changes in the FTIR absorption spectra for various samples

Absorption bands (cm^{-1})	Due to	GO	Chemical reduction						Physical reduction	
			HMG1	HMG2	HMG3	BMG1	BMG2	BMG3	AMG	ACMG
3420	O–H	o	d	d	d	o	o	o	d	d
1730	C=O	o	n/o	n/o	n/o	n/o	n/o	n/o	d	n/o
1629	Water molecules	o	n/o	n/o	n/o	o	d	d	d	d
1552	C–C stretching	n/o	o	o	o	n/o	o	o	o	o
1395	C–OH	o	o	o	o	o	o	o	o	o
1037	C–O	o	o	o	o	o	o	o	o	o

The peak is observed [o], The peak is no observed [n/o]
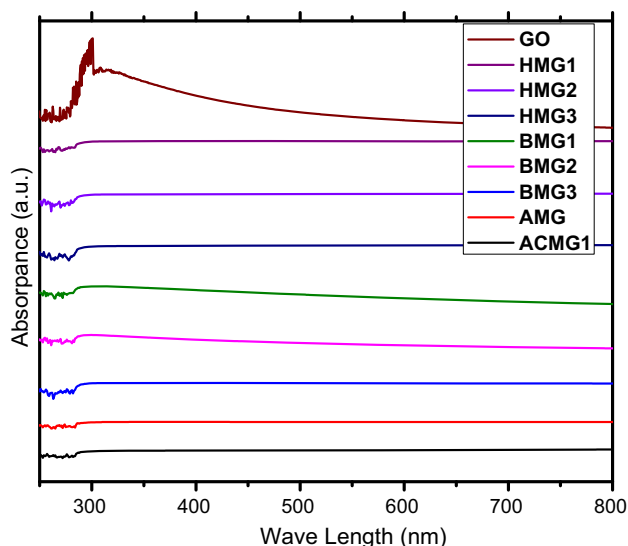
The peak intensity is decreased compared to the GO [d]

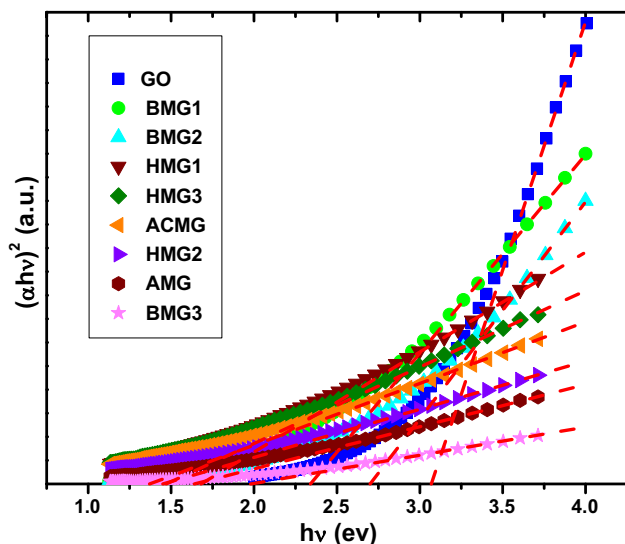**Fig. 7** Ultraviolet–visible absorption spectra of GO and modified graphene sheets

Fig. 9 Band gap obtained by UV–Vis analysis

Fig. 8 Absorption curve in terms of photon energy. The *intersection of the tangent to the curve* and the *horizontal axis* shows the gap

As mentioned oxygen-containing groups on the surface of graphene opens gap in graphene. According to XRD diffraction pattern of ACMG, Fig. 2, after thermal annealing peak at $2\theta \sim 10°$ corresponding to GO has disappeared and a broad peak at $2\theta \sim 26°$ appears. This shows that heat treatment reduces the oxygen-containing groups and thus decreases the gap (Fig. 9). Since according to Scherrer equation [41] the peak width is inversely related to the size of crystalline grains in the sample ACMG, peak broadening shows that thermal annealing reduces the size of the graphene sheets, and thus it caused peak broadening in XRD diffraction pattern. From this perspective, HMG2 sample quality is better than the ACMG. Also, because the thermal annealing only decreased 5 % of gap compared to the gap of HMG2, in practice the cost of production of HMG2 is lower.

4.8 Photoluminescence spectrum

The PL emission spectrum could be attributed to the co-existence of multiple fluorescent centers. These components can be assigned to originate from different defect sites from the surface of the samples such as electron–phonon coupling, lattice dislocation, and the localization of charge carriers due to interface effects. Studies have also suggested that PL in GO and reduced graphene oxide is due to electronic states associated with zigzag edges and chemical species.

The photoluminescence (PL) spectrums for samples were recorded using excitation wavelengths of 255 and 305 nm. The Fig. 10a shows an excitation peak in the near ultraviolet UV region at 255 nm with some emission with

the preparation of graphene. Because at the same time it had a good crystalline structure, and also functional groups were effectively removed from the surface and with the increasing amount of hydrazine hydrate in the sample HMG3 little change had taken place. Although the heat treatment performed on sample, HMG3 reduced the gap, but also caused broadening of the peak in the XRD spectra. In the samples were produced with sodium borohydride treatment, although increasing the amount of sodium borohydride reduced the gap, but also was weaker than hydrazine hydrate.
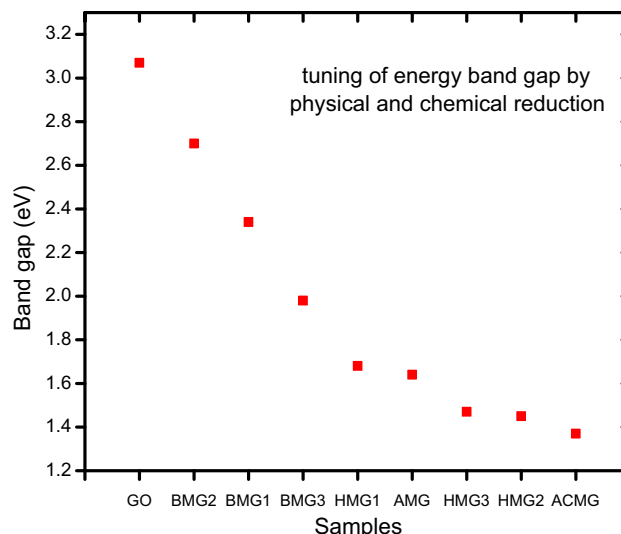
Table 3 A summary results of the various analyzes

Sample	Reduction method	Situation	XRD	FTIR	Band gap (eV)
GO	–	–	A peak at 2θ = 10° due to graphene oxide	A broad peak at 3420 cm^{-1} due to OH	3.07
			A peak at 2θ = 20.1° due to defect the edge areas		
HMG1	Chemical reduction	1 ml hydrazine hydrate per 100 mg GO	Remove of the peak at 2θ = 10° GO	Decrease of broad peak OH compare to GO	1.68
			A peak at 2θ = 20.1°		
HMG2	Chemical reduction	3 ml hydrazine hydrate per 100 mg GO	Remove of the peak GO	Decrease of broad peak OH compare to GO	1.45
			Increase peak at 2θ = 20.1° compared to HMG1		
HMG3	Chemical reduction	6 ml hydrazine hydrate per 100 mg GO	Decrease of the peak GO	Decrease of broad peak OH compare to HMG2	1.47
			Increase peak at 2θ = 20.1° compared to HMG2		
BMG1	Chemical reduction	0.8 g sodium borohydride per 150 mg GO	Decrease of the peak GO	Decrease of broad peak OH compare to GO	2.34
			Remove of peak at 2θ = 20.1°		
BMG2	Chemical reduction	1.2 g sodium borohydride per 150 mg GO	Decrease of the peak GO compared to BMG1	Decrease of broad peak OH compare to BMG1	2.70
			A weak peak at 2θ = 20.1°		
BMG3	Chemical reduction	1.6 g sodium borohydride per 150 mg GO	Decrease of the peak GO compared to BMG2	Decrease of broad peak OH compare to BMG2	1.98
			A weak peak at 2θ = 20.1°		
ACMG	Physical reduction	At 200 °C in the presence of argon	Decrease of the peak GO	Decrease of broad peak OH compare to GO	1.37
			A peak at 2θ = 20.1°		
AMG	Physical reduction	At 200 °C in the presence of argon	Remove of the peak	Decrease of broad peak OH compare to GO	1.64
			Increase peak at 2θ = 20.1° compare to ACMG		

various intensities around 500 nm. The emission strong intensity at 500 nm due to the overlap of the second-order emissions in the electron–hole recombination processes as results from different types of electronically excited states and there is not any fluorescence from the graphene oxide sample [42]. The PL spectrum shown in Fig. 10b was recorded using another excitation wavelength at 305 nm to further explore the PL emission. This time emission peak is observed at 600 nm. However, for both emission wavelengths of 500 and 600 nm, the physical reduction method had minimum of intensity. The observation of PL implies the presence of a band gap in the electronic structure of the graphene various states as a result of the increase in the number of sp^2 carbon atoms in reduction conditions of graphene oxide.

On the other hand, the presence o-bond in a large fraction of sp^3 hybridized carbon atoms bond to oxygen functional groups in graphene sheets cause the formation of islands of graphene in graphene oxide, which produces a disruption of the π-bond and thus opens up a band gap in the electronic structure [42]. It is expected that by controlling the amount of oxidation during synthesis and also reduction can be adjusted the electronic band gap.

5 Conclusion

A systematic approach was used to produce graphene by the chemical and thermal reduction route with various reductants and different concentrations, as well as two different physical reduction methods. In the chemical method, the hydrazine hydrate and sodium borohydride as a reducing agent were used with three different molar concentrations. To produce modified graphene through reducing physical method, two different samples of graphene oxide and chemically reduced graphene oxide in the presence of argon gas at a temperature of 200 °C was used.

The presence of functional groups, its structural properties and morphology were analyzed by FTIR, XRD, scanning electron microscope (SEM), transmission electron microscopy (TEM) and thermo gravimetric analysis (TGA) and photoluminescence (PL).
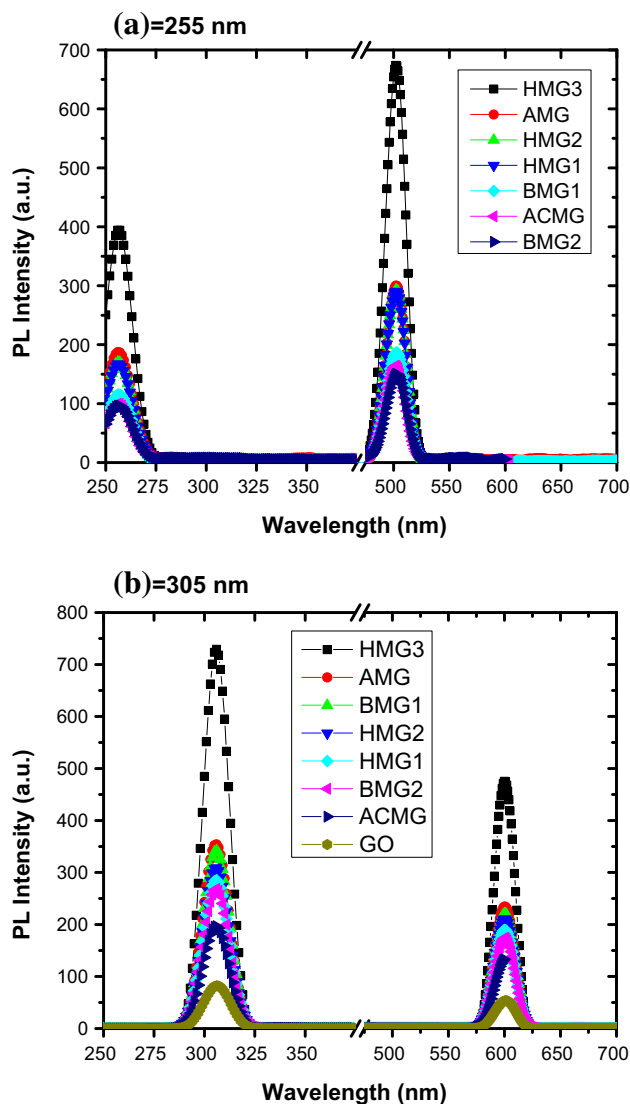
Fig. 10 PL spectrum for GO and modified graphene sheets measured at excitation wavelengths of **a** 255 nm, and **b** 305 nm

Using the analysis characterized results can extract the following conclusions:

- Studies on the results confirmed that the multilayer graphene sheets have been formed in all physical and chemical routes.
- By comparison with other samples showed that modified graphene by hydrazine hydrate treatment (3 ml per 100 mg of GO) has the best structural characteristics among other samples.
- The obtained graphene nano-sheets showed an energy band gap from 1.37 to 2.70 eV.
- Comparison of the spectra of XRD, FTIR and calculation of the band gap samples synthesized by chemical and physical reduction methods show that chemical reduction by hydrazine hydrate removes the

oxygenated groups better compared to the other two methods.

- The physical reduction by heat treatment in the presence of argon gas can effectively remove oxygen groups and cause a reduction in the gap. Due to the low cost, being fast and having no pollution, physical reduction may be more interested in sensing applications and composites.
- Chemical reduction by sodium borohydride eliminated less oxygen groups than the other two methods that shows sodium borohydride is a weaker reducing agent than hydrazine hydrate.
- The PL spectroscopy implies the presence of a band gap in the electronic structure of the graphene various states as a result of the increase in the number of sp^2 carbon atoms in reduction conditions of graphene oxide.
- This method is suggested as an application method for regulation of the energy band gap.

References

1. A.K. Geim, K.S. Novoselov, The rise of graphene. Nat. Mater. **6**, 183–191 (2007)
2. G. Eda, G. Fanchini, M. Chhowalla, Large-area ultrathin films of reduced graphene oxide as a transparent and flexible electronic material. Nat. Nanotechnol. **3**, 270–274 (2008)
3. R. Verdejo, F. Barroso-Bujans, M.A. Rodríguez-Pérez, J.A. de Saja, M.A. López-Manchado, Functionalized graphene sheet filled silicone foam nanocomposites. J. Mater. Chem. **18**, 2221–2226 (2008)
4. F. Schedin, A.K. Geim, S.V. Morozov, E.W. Hill, P. Blake, M.I. Katsnelson, K.S. Novoselov, Detection of individual gas molecules adsorbed on graphene. Nat. Mater. **6**, 652–655 (2007)
5. M.D. Stoller, S. Park, Y. Zhu, J. An, R.S. Ruoff, Graphene-based ultracapacitors. Nano Lett. **8**, 3498–3502 (2008)
6. S. Park, K.-S. Lee, G. Bozoklu, W. Cai, S.T. Nguyen, R.S. Ruoff, Graphene oxide papers modified by divalent ions—enhancing mechanical properties via chemical cross-linking. ACS Nano **2**, 572–578 (2008)
7. C. Lee, X. Wei, J.W. Kysar, J. Hone, Measurement of the elastic properties and intrinsic strength of monolayer graphene. Science **321**, 385–388 (2008)
8. A.A. Balandin, S. Ghosh, W. Bao, I. Calizo, D. Teweldebrhan, F. Miao, C.N. Lau, Superior thermal conductivity of single-layer graphene. Nano Lett. **8**, 902–907 (2008)
9. K.I. Bolotin, K.J.S. Stormer, Z.J.M. Klima, G. Fudenberg, J. Hone, P. Kim, H.L. Stormer, Ultrahigh electron mobility in suspended graphene. Solid State Commun. **146**, 351–355 (2008)
10. M. Eizenberg, J.M. Blakely, Carbon monolayer phase condensation on Ni(111). Surf. Sci. **82**, 228–236 (1970)
11. K.S. Novoselov, Electric field effect in atomically thin carbon films. Science **306**, 666–669 (2004)
12. C. Berger, Electronic confinement and coherence in patterned epitaxial graphene. Science **312**, 1191–1196 (2006)
13. Y. Zhu, S. Murali, W. Cai, X. Li, J.W. Suk, J.R. Potts, R.S. Ruoff, Graphene and graphene oxide: synthesis, properties, and applications. Adv. Mater. **22**(35), 3906–3924 (2010)

14. B.C. Brodie, Sur le poids atomique du graphite. Ann. Chim. Phys. **56**, 466 (1860)

15. L. Staudenmaier, Verfahren zur Darstellung der Graphitsaure. Ber. Deut. Chem. Ges. **31**, 1481 (1898)

16. W.S. Hummers, R.E. Offeman, Preparation of graphitic oxide. J. Am. Chem. Soc. **80**, 1339 (1958)

17. D.C. Marcano, D.V. Kosynkin, J.M. Berlin, A. Sinitskii, Z. Sun, A. Slesarev, L.B. Alemany, W. Lu, J.M. Tour, Improved synthesis of graphene oxide. ACS Nano **4**(8), 4806–4814 (2010)

18. A. Buchsteiner, A. Lerf, J. Pieper, Water dynamics in graphite oxide investigated with neutron scattering. J. Phys. Chem. B **110**, 22328–22338 (2006)

19. I. Jung, M. Pelton, R. Piner, D.A. Dikin, S. Stankovich, S. Watcharotone, M. Hausner, R.S. Ruoff, Simple approach for high-contrast optical imaging and characterization of graphene-based sheets. Nano Lett. **7**, 3569–3575 (2007)

20. Y. Xu, H. Bai, G. Lu, C. Li, G. Shi, Flexible graphene films via the filtration of water-soluble noncovalent functionalized graphene sheets. J. Am. Chem. Soc. **130**, 5856–5857 (2008)

21. J.R. Lomeda, C.D. Doyle, D.V. Kosynkin, W.-F. Hwang, J.M. Tour, Diazonium functionalization of surfactant-wrapped chemically converted graphene sheets. J. Am. Chem. Soc. **130**, 16201–16206 (2008)

22. R. Muszynski, B. Seger, P.V. Kamat, Decorating graphene sheets with gold nanoparticles. J. Phys. Chem. C **112**, 5263–5266 (2008)

23. M.J. McAllister, J.-L. Li, D.H. Adamson, H.C. Schniepp, A.A. Abdala, J. Liu, M. Herrera-Alonso, D.L. Milius, R. Car, R.K. Prud'homme, Single sheet functionalized graphene by oxidation and thermal expansion of graphite. Chem. Mater. **19**, 4396–4404 (2007)

24. S. Stankovich, D.A. Dikin, R.D. Piner, K.A. Kohlhaas, A. Kleinhammes, Y. Jia, Y. Wu, S.T. Nguyen, R.S. Ruoff, Synthesis of graphene-based nanosheets via chemical reduction of exfoliated graphite oxide. Carbon **45**(7), 1558–1565 (2007)

25. W. Gao, L.B. Alemany, L. Ci, P.M. Ajayan, New insights into the structure and reduction of graphite oxide. Nat. Chem. **1**(5), 403–408 (2009)

26. X. Gao, J. Jang, S. Nagase, Hydrazine and thermal reduction of graphene oxide: reaction mechanisms, product structures, and reaction design. J. Phys. Chem. C **114**(2), 832–842 (2009)

27. Y. Wu, B. Wang, Y. Ma, Y. Huang, N. Li, F. Zhang, Y. Chen, Efficient and large-scale synthesis of few-layered graphene using an arc-discharge method and conductivity studies of the resulting films. Nano Res. **3**(9), 661–669 (2010)

28. Z.Q. Li, C.J. Lu, Z.P. Xia, Y. Zhou, Z. Luo, X-ray diffraction patterns of graphite and turbostratic carbon. Carbon **45**, 1686–1695 (2007)

29. E.H.L. Falcao, R.G. Blair, J.J. Mack, L.M. Viculis, C.W. Kwon, M. Bendikov, R.B. Kaner, B.S. Dunn, F. Wudl, Microwave exfoliation of a graphite intercalation compound. Carbon **45**, 1367–1369 (2007)

30. X. Zhang, K. Li, H. Li, J. Lu, Q. Fu, Y. Chu, Graphene nanosheets synthesis via chemical reduction of graphene oxide using sodium acetate trihydrate solution. Synth. Met. **193**, 132–138 (2014)

31. J. Shen, T. Li, Y. Long, M. Shi, N. Li, M. Ye, One-step solid state preparation of reduced graphene oxide. Carbon **50**(6), 2134–2140 (2012)

32. C.D. Zangmeister, Preparation and evaluation of graphite oxide reduced at 220 °C. Chem. Mater. **22**, 5625–5629 (2010)

33. J.I. Paredes, S. Villar-Rodil, A. Martínez-Alonso, J.M.D. Tascón, Graphene oxide dispersions in organic solvents. Langmuir **24**, 10560–10564 (2008)

34. G. Venugopal, K. Krishnamoorthy, R. Mohan, S.-J. Kim, An investigation of the electrical transport properties of graphene-oxide thin films. Mater. Chem. Phys. **132**(1), 29–33 (2012)

35. K. Krishnamoorthy, M. Veerapandian, K. Yun, S.-J. Kim, The chemical and structural analysis of graphene oxide with different degrees of oxidation. Carbon **53**, 38–49 (2013)

36. H. Liu, Y. Liu, D. Zhu, Chemical doping of graphene. J. Mater. Chem. **21**(10), 3335 (2011)

37. S. Yang, W. Yue, D. Huang, C. Chen, H. Lin, X. Yang, A facile green strategy for rapid reduction of graphene oxide by metallic zinc. RSC Adv. **2**(23), 8827–8832 (2012)

38. K. Krishnamoorthy, R. Mohan, S.-J. Kim, Graphene oxide as a photocatalytic material. Appl. Phys. Lett. **98**(24), 244101 (2011)

39. S. Safa, R. Sarraf-Mamoory, R. Azimirad, Investigation of reduced graphene oxide effects on ultra-violet detection of ZnO thin film. Phys. E Low-dimens. Syst. Nanostruct. **57**, 155–160 (2014)

40. H.-C. Hsu, I. Shown, H.-Y. Wei, Y.-C. Chang, H.-Y. Du, Y.-G. Lin, C.-A. Tseng, C.-H. Wang, L.-C. Chen, Y.-C. Lin, Graphene oxide as a promising photocatalyst for CO2 to methanol conversion. Nanoscale **5**(1), 262–268 (2012)

41. A. Monshi, M.R. Foroughi, M.R. Monshi, Modified Scherrer equation to estimate more accurately nano-crystallite size using XRD. World J. Nanosci. Eng. **2**, 154–160 (2012)

42. S. Shukla, S. Saxena, Spectroscopic investigation of confinement effects on optical properties of graphene oxide. Appl. Phys. Lett. **98**(7), 73104 (2011)